Direction-dependent optical solitary waves in nematic liquid crystals

Enrique Calisto and Gaetano Assanto

Phys. Rev. A **108**, 043509 — Published 17 October 2023

DOI: 10.1103/PhysRevA.108.043509

Direction-dependent optical solitary waves in nematic liquid crystals

Enrique Calisto[1] and Gaetano Assanto[2]

[1]*School of Mathematics, University of Edinburgh, Edinburgh EH9 3FD, Scotland, U.K.*
[2]***NooEL**— Nonlinear Optics and OptoElectronics Lab, University "Roma Tre", 00146 Rome, Italy*

We investigate the optical propagation of reorientational solitary waves in non-uniformly oriented planar samples of thermo-tropic liquid crystals in the nematic phase. A non-symmetric distribution of the optic axis, across either the longitudinal or transverse coordinates, entails nematicon paths affected by the side of the cell where the excitation is launched, i.e., direction-sensitive trajectories. We analyze the effect with reference to realistic samples encompassing a linearly modulated orientation vs either length or width, presenting nonlinear models and the outcome of numerical experiments. We briefly discuss the resulting non-specular transmission in terms of optical non-reciprocity and isolation.

PACS numbers: 42.65.Tg, 42.70.Df, 05.45.Yv

I. INTRODUCTION

In the last few decades [1], thermotropic liquid crystals in the nematic mesophase (NLC) have been employed as an ideal anisotropic dielectric for studying various nonlinear optical phenomena related to polarization as well as intensity dependent responses to electromagnetic wavepackets at optical frequencies, including modulational instability, random lasing, spatial solitons and shock waves [2–12]. In particular, spatial solitary waves in nematic liquid crystals, usually referred to as "Nematicons" [1, 13, 14], are stable and robust self-confined beams which can propagate diffractionless within the light-induced channel waveguide, typically wider than the optical wavepacket owing to a highly nonlocal response [15, 16]. The latter prevents catastrophic collapse and mediates long-range interactions between nonlinear beams [17, 18]. Since nematicons can be launched at milliWatt power levels from light beams in planar geometries allowing for a nematic phase, they have been the subject of several enlightening investigations, including waveguiding and collisions, bistability and hysteresis, reconfigurability and negative refraction, voltage/magnetic steering control, to mention a few effects of interest for soliton fundamental science as well as potential applications [13, 14]. On the theoretical domain, nematicons are described by nonlinear dispersive-wave equations -modelled by a nonlinear Schrödinger-like equation for the propagating envelope- and an elliptic equation for the reorientational response -due to the electric-field torque applied onto the anisotropic molecular dipoles in a liquid state [19].

Nematicons in reorientational NLC are extraordinarily polarized ($e-$) wavepackets self-guided via the all-optical increase of the $e-$refractive index. Although optical wavepackets, including solitary waves, are expected to propagate straight in homogeneous isotropic dielectrics, their trajectory in highly nonlocal and birefringent liquid crystals is determined and can be controlled by the distribution of the optic axis, e.g., by introducing local/nonlocal perturbations or modulations of its angular orientation, including defects, interfaces or lens-like regions [13, 14, 19]. Since the optic axis $\vec{n}$ of the equivalent uniaxial corresponds to the NLC molecular director, its spatial distribution can be engineered by suitable anchoring at the confining interfaces or by the use of external means. The angular orientation of $\vec{n}$ with respect to the beam wave-vector $\vec{k}$ locally determines both the index of refraction n_e and the walk-off angle δ between $\vec{k}$ and the Poynting vector $\vec{s}$ of $e-$waves.

When considering a standard geometry, i. e., a planar NLC cell with input and output interfaces/ports for the light beam separated by a propagation distance L, the all-optical response (supporting solitary waves) in the presence of a non-symmetric dis-homogeneity or modulation (giving rise to a distribution of index and walk-off) can translate into non-specular beam paths when identical excitations are launched from opposite sides. The latter direction-dependent response is one of the mechanisms exploited for passive nonlinear isolators, such as those based on degenerate three-photon interactions or Kerr directional coupling [20, 21].

In this Paper, inspired by the diode-like behaviour of previously demonstrated non-symmetric nonlinear optical configurations [20] and previous reports on bent nematicons in NLC with non-uniform anchoring [22, 23], we analyze the direction-dependence of nematicon beams and waveguides excited in planar NLC cells with angular orientation of the optic axis being modulated along either the longitudinal or the transverse coordinate. We conduct numerical experiments to investigate the evolution and trajectories of solitary waves launched from opposite sides of the cell, specifically their amplitudes, profiles and transverse separation when forward-propagating (FP) output and backward-propagating (BP) input locations coincide. We briefly discuss non-specular transmission of self-confined and guided-waves in terms of reciprocity and optical isolation.

II. MODEL

We examine geometries in planar cells of length L, width d and thickness h ($h \ll d, L$) along z, y and x, respectively, with (x, y, z) a standard system of mutually orthogonal Cartesian axes. We assume the positive uniaxial NLC to be prepared in the nematic mesophase with an order parameter close to unity and molecular director $\vec{n}$ oriented in (y, z), the principal plane where the electric field, wave-vector $\vec{k}$ and Poynting-vector $\vec{s}$ of extraordinary-polarized light lay. Here we denote by θ the orientation angle between $\vec{k}$ and $\vec{n}$ and by δ the walk-off between $\vec{s}$ and $\vec{k}$, respectively. Throughout this study, in the linear regime $\theta = \theta(y, z)$, whereas the nonlinear reorientation $\psi = \psi(x, y, z)$ induced by an e-beam is a small perturbation to θ, with the overall orientation being $\Theta = \theta + \psi$ and $\psi \ll \theta$.
Nematicons stem from the robust balance between linear diffraction and nonlinear e-index increase $n_e = n_e[\Theta(x, y, z)] \approx n_e[\theta(y, z)] + \psi dn_e(\theta)/d\theta$ in the planar geometries of interest and in the presence of a nonlocal and saturable all-optical response. The latter givers rise to graded-index channel waveguides featuring large numerical aperture and able to confine e-polarized signals, with (energy flux) propagation at angle δ with respect to the input wave-vector. It is convenient to recall from the optics of uniaxial media that

$$n_e(\theta) = \frac{n_\perp n_\parallel}{\left[\left(n_\perp^2 - n_\parallel^2\right)\sin^2\theta + n_\parallel^2\right]^{1/2}}, \tag{1}$$

$$\delta(\theta) = -\frac{1}{n_e(\theta)}\frac{dn_e(\theta)}{d\theta}, \tag{2}$$

being $c_0/n_\perp (c_0/n_\parallel)$ the ordinary-wave (extraordinary wave) phase-velocity eigenvalue (here c_0 denotes the speed of light in vacuum). We define the optical anisotropy $\Delta\epsilon = n_\parallel^2 - n_\perp^2$ and $\Delta = \tan\delta$, such that

$$\Delta(\Theta) = \frac{\Delta\epsilon \sin 2\Theta}{\Delta\epsilon + 2n_\perp^2 + \Delta\epsilon\cos 2\Theta}, \tag{3}$$

accounting for the nonlinear perturbation, as well.
For a light beam polarized as an extraordinary-wave and propagating along z, in the paraxial approximation with an injected component $E = E_y$ of the electric field and neglecting $E_z \ll E_y$, assuming transverse confinement across x in the solitary-wave regime [24], the evolution of the envelope E in the principal plane (y, z) is ruled by the nonlinear Schrödinger-type equation:

$$2ik_0 n_e\left(\frac{\partial E}{\partial z} + \Delta(\Theta)\frac{\partial E}{\partial y}\right) + \frac{\partial^2 E}{\partial y^2} + k_0^2(n_\perp^2\cos^2\Theta)E$$
$$+k_0^2\left(n_\parallel^2\sin^2\Theta - n_\perp^2\cos^2\theta_0 - n_\parallel^2\sin^2\theta_0\right)E = 0. \tag{4}$$

Equation 4 needs to be coupled to the NLC reorientation model, which can be obtained from the minimization of the Frank-Oseen energy density as the Euler-Lagrange equation

$$K_{22}\frac{\partial^2\Theta}{\partial x^2} + (K_{11}\cos^2\Theta + K_{33}\sin^2\Theta)\frac{\partial^2\Theta}{\partial y^2}$$
$$-\frac{1}{2}\sin 2\Theta(K_{11} - K_{33})\left(\frac{\partial\Theta}{\partial y}\right)^2 + \frac{\epsilon_0\Delta\epsilon}{2}\left[\sin 2\Theta E^2\right] = 0$$

with K_{11}, K_{22} and K_{33} the Frank elastic constants for splay, twist and bend deformations in the distribution of the molecular director $\vec{n} = (0, \sin\Theta, \cos\Theta)$ in the specific (1+1)D geometry under consideration. In the single constant approximation whereby the elastic deformations are taken equal, i. e., $K_{11} = K_{22} = K_{33} = K$, the Euler-Lagrange equation above can be recast as

$$K\frac{\partial^2\Theta}{\partial y^2} + \frac{1}{4}\epsilon_0\Delta\epsilon|E|^2\sin 2\Theta = 0. \tag{5}$$

The nematicon model Eqs. (4-5) are hard to solve in general [25]. In the frame of the first-order perturbation theory, taking the all-optical reorientation ψ to be much smaller than the background orientation θ and expanding the trigonometric functions, Eqs. (4-5) reduce to

$$2ik_0 n_e\left(\frac{\partial E}{\partial z} + \Delta(\Theta)\frac{\partial E}{\partial y}\right) + \frac{\partial^2 E}{\partial y^2}$$
$$+k_0^2\Delta\epsilon\left[\sin^2\theta - \sin^2\theta_0 + \sin(2\theta)\,\psi\right]E = 0, \tag{6}$$
$$K\frac{\partial^2\psi}{\partial y^2} + \frac{1}{4}\epsilon_0\Delta\epsilon|E|^2\sin(2\theta) = 0. \tag{7}$$

In this Paper we consider the simple cases of either a purely longitudinal modulation $\theta = \theta(z)$ or a purely transverse modulation $\theta = \theta(y)$. In the former limit, using the phase transformation

$$E \to E\exp\left(\frac{ik_0}{2n_e}\int_0^z \left\{\Delta\epsilon(\sin^2\theta - \sin^2\theta_0)\right\}du\right) \tag{8}$$

the electric field equation becomes

$$2ik_0 n_e\left[\frac{\partial E}{\partial z} + \Delta(\Theta)\frac{\partial E}{\partial y}\right] + \frac{\partial^2 E}{\partial y^2} + k_0^2\Delta\epsilon\left[\sin(2\theta)\right]\psi E = 0.$$

We introduce the dimensionless coordinates (Y, Z)

$$y = \frac{\lambda}{\pi\sqrt{\Delta\epsilon\sin 2\theta_0}}Y, \quad z = \frac{2n_e\lambda}{\pi\Delta\epsilon\sin 2\theta_0}Z$$

and the unitless amplitude u of the electric field envelope

$$E = \sqrt{\frac{4P_b}{\pi\epsilon_0 c n_e W_b^2}}u \tag{9}$$

in order to get

$$i\frac{\partial u}{\partial Z}+i\gamma\Delta(\Theta)\frac{\partial u}{\partial Y}+\frac{1}{2}\frac{\partial^2 u}{\partial Y^2}+2\frac{\sin(2\theta(Z))}{\sin(2\theta(0))}\psi u=0 \quad (10)$$

$$\nu\frac{\partial^2\psi}{\partial Y^2}+2\frac{\sin(2\theta(Z))}{\sin(2\theta(0))}|u|^2=0 \quad (11)$$

with λ the wavelength. For this case $\theta=\theta(z)$ we also define the walk-off coefficient γ and elasticity parameter ν as

$$\gamma=\frac{2n_e}{\sqrt{\Delta\epsilon\sin(2\theta(0))}},\quad \nu=\frac{2\pi^3 c n_e K W_b^2}{\lambda^2 P_b}. \quad (12)$$

The non-dimensionalization above is based on a reference Gaussian beam of power P_b and half-width W_b, whose values are taken as $P_b = 2.7mW$ and W_b=3.5 μm, respectively, consistently with typical experimental parameters.

When $\theta=\theta(y)$, i. e., in a planar cell with orientation modulation in the transverse coordinate only, the electric field transformation Eq. (8) cannot be applied, and the dimensionless model is then

$$i\frac{\partial u}{\partial Z}+i\gamma\Delta(\Theta)\frac{\partial u}{\partial Y}+\frac{1}{2}\frac{\partial^2 u}{\partial y^2}$$
$$+\left[\sin^2\theta(Y)-\sin^2\theta_0+\sin(2\theta(Y))\,\psi\right]u = 0, \quad (13)$$

$$\nu\frac{\partial^2\psi}{\partial Y^2}+2\left[\sin\left(2\theta(Y)\right)\right]|u|^2 = 0. \quad (14)$$

Here, at variance with Eq. (12),

$$\nu=\frac{2\pi^3 c n_e K W_b^2}{\lambda^2 P_b},\quad \gamma=\frac{2n_e}{\sqrt{\Delta\epsilon}}. \quad (15)$$

In the numerical experiments we adopted material parameters typical of the NLC mixture E7, with $n_\parallel = 1.7$, $n_\perp = 1.5$ and $K = 1.2\times10^{11}N$, with elasticity/nonlocality $\nu = 250$. We considered a planar cell of size $(h,d,L)=(30,600,1000)\mu m$, Gaussian beams of wavelength $1064nm$ in the extraordinary polarization launched forward in $(y_0,0)$ or backward in $(y_{FP}(L),L)$, with $y_{FP}(L)$ the transverse position of the outgoing FP wavepacket. The electric field equation was solved in Y using the Fast-Fourier Transform and propagated in Z using a 4th-order Runge-Kutta scheme.

III. LINEAR LONGITUDINAL MODULATION

First, we consider a planar cell where the background orientation (at rest) has a linear dependence across the length L of the NLC sample and is uniform across the width, with $\theta_0=\theta(z=0)$ and $\theta_L=\theta(z=L)$. As in a preliminary report [23], we launched identical input beams with $\vec{k}=\vec{z}$ for forward propagation (FP) and $\vec{k}=-\vec{z}$ for backward propagation (BP), using the reference values of beam power, width and wavelength to ensure the formation and propagation of nematicons throughout this study. For a linear variation from $\theta_0=10^\circ$ to $\theta_L=45^\circ$, Fig. 1(a) displays the refractive index $n_e(z)$ and walkoff $\delta(z)$ distributions in the cell, whereas Fig. 1(b-d) graphs the resulting FP and BP nematicon transverse profiles (input, FP output, BP output), their amplitude

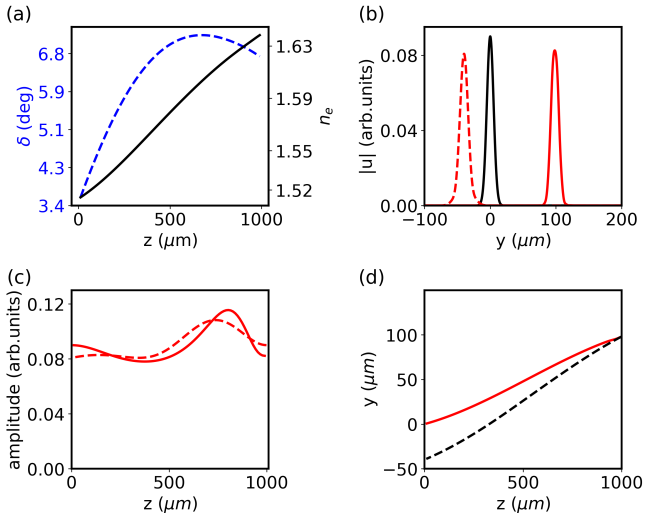

FIG. 1: Linear longitudinal modulation from $\theta_0=10^\circ$ to $\theta_L=45^\circ$. (a) Refractive index $n_e(z)$ (black) and angular walkoff $\delta(z)$ (blue dashes) versus z in a $1mm$-long cell filled with E7. (b) Transverse profiles of input (black solid line), FP (red solid line) and BP transmitted (red dashes) wavepackets. (c) Amplitudes of FP (solid line) and BP (dashed line) nematicons versus z. (d) Trajectories of FP (solid line) and BP (dashed line) nematicons in y,z.

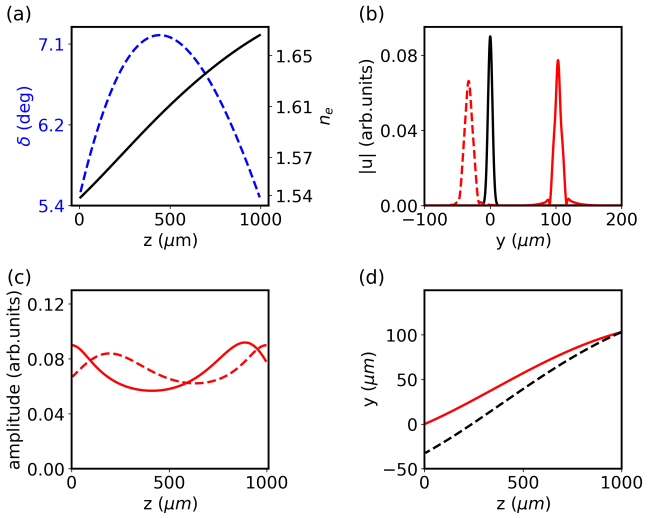

FIG. 2: Linear longitudinal modulation from $\theta_0=20^\circ$ to $\theta_L=60^\circ$. (a) Refractive index $n_e(z)$ (black) and walkoff $\delta(z)$ (blue dashes) distributions. (b) Profiles of input, FP and BP outputs. (c) Amplitudes of FP (solid line) and BP (dashes) solitons versus propagation. (d) Trajectories of FP (red solid line) and BP (black dashes) nematicons.

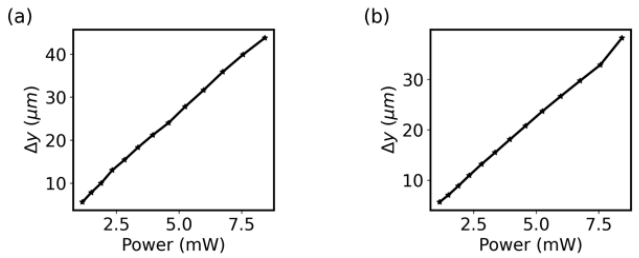

FIG. 3: Linear longitudinal modulation. Beam power dependence of transverse separation Δy for (a) $\theta_0 = 10^\circ$ to $\theta_L = 45^\circ$; (b) $\theta_0 = 20^\circ$ to $\theta_L = 60^\circ$. Dots are calculated points, lines are guides to the eye.

evolution (linked to their width via the transverse profile as ideal nematicons conserve power) and trajectories versus z, respectively. It is apparent that, owing to the nonlinear response in the absence of mid-cell symmetry, the z-modulated responses in nonlinearity and walkoff result in distinct evolution of the FP wavepacket as compared to the BP wavepacket, with the BP output location well separated from the FP input $y = 0$ and $\Delta y = y_{BP}(0) - y_{FP}(0) \approx 50\mu m$, well in excess of the nematicon spotsize. Fig 2(a-d) illustrates the case of modulation from $\theta_0 = 20^\circ$ to $\theta_L = 60^\circ$, with $\Delta y \approx 40\mu m$. Finally, while the transverse separation Δy is zero in the linear limit ($\psi = 0$), it is a function of the input power in the reorientational regime, as plotted in Fig. 3(a-b) for two different intervals of linearly varying orientation $\theta(z)$.

IV. LINEAR TRANSVERSE MODULATION

While in the previous section nematicons launched from opposite sides of the samples underwent different (linear as well as power-dependent) walkoff, in an NLC sample with orientation modulation in the transverse coordinate y, both walkoff and refraction act on the wavepackets, as they propagate through regions with modulated refraction. Fig. 4(a-d) shows the refractive index $n_e(y)$ and walkoff $\delta(y)$ distributions in a y-modulated cell with orientation linearly modulated from $\theta_{bot} = 65^\circ$ to $\theta_{top} = 25^\circ$ across the width d and an FP input launched in $(y_0, z) = (100\mu m, 0)$ with $\theta(y_0) = 38^\circ$. In this case (see also Ref. [22]) refraction and walkoff tend to counteract their effects on the FP beam, whereas they act synergistically on the BP wavepacket, with a resulting $\Delta y \approx -180\mu m$. Fig. 5(a-d) displays another case, where the orientation goes from $\theta_{bot} = 25^\circ$ to $\theta_{top} = 65^\circ$ and the FP beam is launched in $(y_0, z) = (-200\mu m, 0)$ with $\theta(y_0) = 32^\circ$ and $\Delta y \approx 180\mu m$. Fig. 6(a-b) illustrates the corresponding power dependence of Δy.

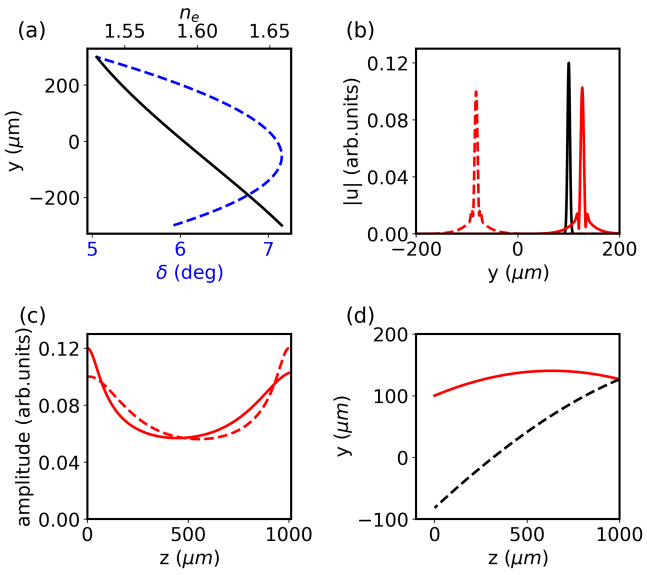

FIG. 4: Linear transverse modulation from $\theta_{bot} = 65^\circ$ to $\theta_{top} = 25^\circ$ across a cell width $d = 600\mu m$. (a) Refractive index $n_e(y)$ (black) and angular walkoff $\delta(y)$ (blue dashes) in a $1mm$-long cell. (b) Transverse profiles of input (black solid line), FP (solid red) and BP output (dashed red) wavepackets. (c) Amplitudes of FP (solid line) and BP (dashed line) nematicons. (d) Trajectories of FP (red solid line) and BP (black dashes) nematicons.

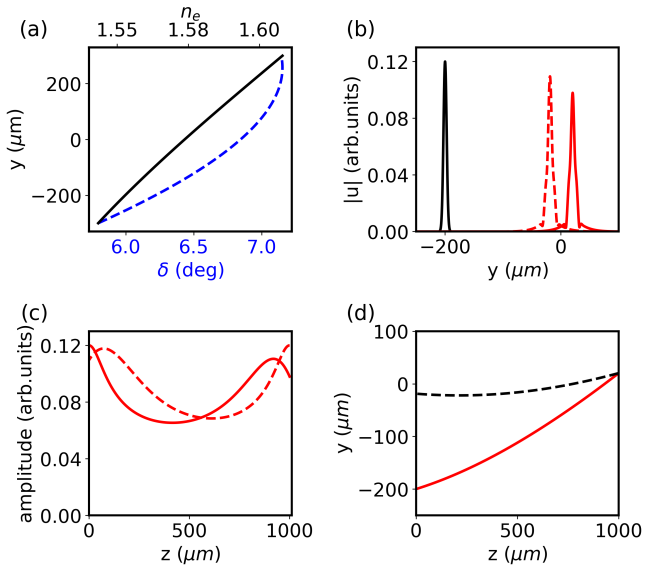

FIG. 5: Linear transverse modulation from $\theta_{bot} = 25^\circ$ to $\theta_{top} = 65^\circ$ across $d = 600\mu m$. (a) Refractive index $n_e(y)$ (black) and angular walkoff $\delta(y)$ (blue dashes). (b) Transverse profiles of input (black solid line), FP (red solid line) and BP (red dashes) outputs. (c) Amplitudes of FP (solid line) and BP (dashed line) nematicons. (d) Trajectories of FP (red solid line) and BP (black dashes) nematicons.

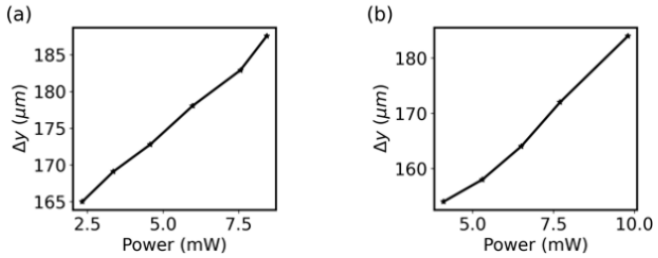

FIG. 6: Linear transverse modulation. Beam power dependence of transverse separation Δy for (a) $\theta_{bot} = 25°$ to $\theta_{top} = 65°$; (b) $\theta_{bot} = 65°$ to $\theta_{top} = 25°$. Dots are calculated, lines are guides to the eye.

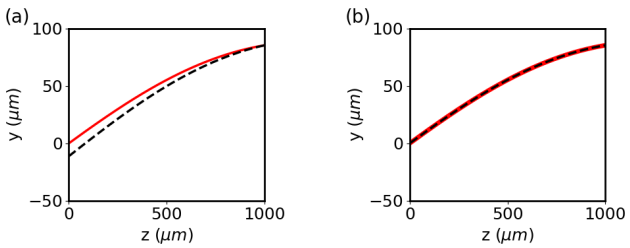

FIG. 7: Linear longitudinal modulation in a sample with $\theta_0 = 45°$ and $\theta_L = 70°$. FP (red solid line) and BP (black dashes) trajectories for (a) identical counter-launched input beams; (b) phase-conjugated reflection: the BP-input is phase-conjugated with respect to the FP output.

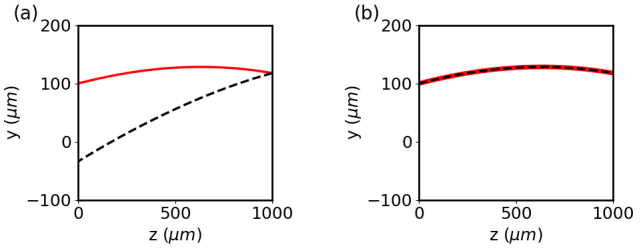

FIG. 8: Linear transverse modulation in a cell with $\theta_{bot} = 75°$ and $\theta_{top} = 45°$. FP (red solid line) and BP (black dashes) trajectories for (a) identical counter-launched input beams, (b) phase-conjugated reflection.

V. DISCUSSION

The simple layout we examined hereby can be regarded as a two-port guided-wave device, in which forward and backward $e-$signals are confined in the nematicon waveguides excited by counter-propagating beams of equal powers and profiles. In this respect, since the BP output signal (nematicon) does not superpose with the FP input signal (nematicon), these NLC cells could be regarded as optical isolators or diodes, with low signal crosstalk and high rejection depending on the separation ($\Delta y \gg W_b$) and adjustable with power and/or orientation modulation. Since the phenomenon rests essentially on the non-specular distribution θ of the optic axis with respect to input and output ports, the description of the NLC samples in terms of a dielectric stack would result into an asymmetric dielectric tensor [26]. Moreover, the self-focusing response associated to reorientation is at the origin of nematicon formation and soliton waveguides. Hence, according to R.J. Potton (Ref. [27]) as well as A.T. de Hoop (Ref. [28]), the previous considerations support the claim of a non-reciprocal transmission despite the passive and non-magnetic character of the (undoped) nematic liquid crystals. While reciprocity and non-reciprocity are more often addressed in the absence of confinement and nonlinear effects, the effect described hereby does not belong to the class of those scattering configurations where inverting the sign of wave-vectors and exchanging source(s) and detector(s) lead to the same transmission, qualifying them as reciprocal [26]. Nevertheless, reciprocity and time-reversal are often used interchangeably; to verify whether the modulated NLC samples satisfy time-reversibility, we repeated the numerical experiments above in the limit of phase-conjugated reflection, i. e., using for the BP input the FP output after phase-conjugation. The results, shown in two instances of $z-$ and $y-$modulated orientation in Fig.7 and Fig.8, respectively, demonstrate that, albeit seemingly non-reciprocal, what we reported is actually time-reversible. Finally, in terms of potential applications of non-reciprocal systems to isolation, the studied configurations lend themselves to optical isolators as qualified by Jalas *et alia* in Ref. [[29]]. The confinement of copolarized signals afforded by reorientational solitary waves in NLC allows the device defined by the two ports in $(y_{FP}(0), 0)$ and $(y_{FP}(L), L)$ to operate as a (nonlinear) optical diode, which transmits forward to port 2 $(y_{FP}(L), L)$ only FP signals injected in port 1 $(y_{FP}(0), 0)$ while isolating port 1 from signals launched in port 2. Moreover, this diode-like operation, consistently with the use of guided-signals, would not be affected by dynamic reciprocity [30].

VI. CONCLUSIONS

We addressed formation and propagation of optical spatial solitons in orientation-modulated nematic liquid crystals, nematicons, outlining their direction-sensitive evolutions and trajectories when launched from opposite sides of non-specular samples. The reported layout is time reversible but, owing to nonlinear and asymmetric dielectric responses, lacks reciprocity and yields optical isolation between counterpropagating signals copolarized with and confined by nematicons. Simple linear variations of the background orientation of the molecular director were presented and discussed using a simplified (1+1) dimensional model; (2+1)D propagation as well as more complex functional forms of orientation modulation are being considered and will be reported elsewhere.

VII. ACKNOWLEDGMENTS

E. C. acknowledges ANID's support (Chile) through Beca Doctorado Extranjero 2020 (72210165). This material is based upon work supported by the Air Force Office of Scientific Research under award no FA8655-23-1-7026.

[1] This paper is dedicated to Noel Frederick Smyth, Professor of Nonlinear Waves at the School of Mathematics, University of Edinburgh. Prof. Smyth passed away prematurely while supervising the first author's research work and collaborating with the second author. His numerous and enthusiastic contributions to nonlinear and solitary waves in liquid crystalshave been of great impact in their theoretical understanding.

[2] I.C. Khoo, "Nonlinear optics of liquid crystalline materials," *Phys. Rep.,* **471**, 2009, 221–267 (2009).

[3] A. E. Miroshnichenko, E. Brasselet and Yu. S. Kivshar, "Light-induced orientational effects in periodic photonic structures with pure and dye-doped nematic liquid crystal defects," *Phys. Rev. A,* **78**, 053823 (2008).

[4] J. Beeckman, X. Hutsebaut, M. Haelterman and K. Neyts, "Induced modulation instability and recurrence in nematic liquid crystals," *Opt. Express,* **15**, 11185–11195 (2007).

[5] G. Strangi, S. Ferjani, V. Barna, A. De Luca, N. Scaramuzza, C. Versace, C. Umeton and R. Bartolino, "Random lasing and weak localization of light in dye-doped nematic liquid crystals," *Opt. Express,* **14**, 7737–7744 (2006).

[6] M.A. Karpierz, "Solitary waves in liquid crystalline waveguides," *Phys. Rev. E,* **66**, 036603 (2002).

[7] M. Peccianti and G. Assanto, "Nematic Liquid Crystals: a suitable medium for self-confinement of coherent and incoherent light," *Phys. Rev. E,* **65**, 035603–035606(R) (2002).

[8] M. Warenghem, J.F. Blach and J.F. Henninot, "Thermo-nematicon: an unnatural coexistence of solitons in liquid crystals?," *J. Opt. Soc. Amer. B,* **25**, 1882–1887 (2008).

[9] A. Ramaniuk, P.S. Jung, D.N. Christodoulides, W. Krolikowski and M. Trippenbach, "Absorption-mediated stabilization of nonlinear propagation of vortex beams in nematic liquid crystals," *Opt. Commun.,* **451**, 338–344 (2019).

[10] S. Perumbilavil, A. Piccardi, R. Barboza, O. Buchnev, G. Strangi, M. Kauranen and G. Assanto "Beaming random lasers with soliton control," *Nature Comm.,* **9**, 3863 (2018).

[11] G. Assanto and N.F. Smyth, "Spin-optical solitons in liquid crystals," *Phys. Rev. A,* **102**, 033501 (2020).

[12] S. Baqer, D.J. Frantzeskakis, T.P. Horikis, C. Houdeville, T.R. Marchant and N.F. Smyth, "Nematic Dispersive Shock Waves from Nonlocal to Local," *Appl. Sci.,* **11**, 4736 (2021).

[13] M. Peccianti and G. Assanto, "Nematicons," *Phys. Rep.,* **516**, 147–208 (2012).

[14] G. Assanto, "Nematicons: reorientational solitons from optics to photonics," *Liq. Cryst. Rev.,* **6**, 170–194 (2018).

[15] C. Conti, M. Peccianti and G. Assanto, "Route to nonlocality and observation of accessible solitons," *Phys. Rev. Lett.,* **91**, 073901 (2003).

[16] C. Conti, M. Peccianti and G. Assanto, "Observation of optical spatial solitons in a highly nonlocal medium," *Phys. Rev. Lett.,* **92**, 113902 (2004).

[17] O. Bang, W. Krolikowski, J. Wyller and J. Rasmussen, "Collapse arrest and soliton stabilization in nonlocal nonlinear media," *Phys. Rev. E,* **66**, 046619 (2002).

[18] M. Peccianti, A. Fratalocchi and G. Assanto, "Transverse dynamics of Nematicons," *Opt. Express.,* **12**, 6524–6529 (2004).

[19] G. Assanto and N. F. Smyth, "Self-confined light waves in nematic liquid crystals," *Physica D,* **402**, 132182 (2020).

[20] K. Gallo, G. Assanto, K. R. Parameswaran and M. M. Fejer, "All-optical diode in a periodically-poled Lithium Niobate waveguide," *Appl. Phys. Lett.,* **79**, 314–316 (2001).

[21] A. Alberucci and G. Assanto, "All-optical isolation by directional coupling," *Opt. Lett.,* **36**, 1641–1643 (2008).

[22] U. Laudyn, M. Kwasny, F. Sala, M. Karpierz, N. F. Smyth and G. Assanto, "Curved solitons subject to transverse acceleration in reorientational soft matter," *Sci. Rep.,* **7**, 12385 (2017).

[23] E. Calisto, N. F. Smyth and G. Assanto, "Optical isolation via direction-dependent soliton routing in birefringent soft-matter," *Opt. Lett.,* **47**, 459564 (2022).

[24] A. Alberucci and G. Assanto, "Nematicons beyond the perturbative regime," *Opt. Lett.,* **35**, 2520—2522 (2010).

[25] J. M. L. MacNeil, N. F. Smyth and G. Assanto, "Exact and approximate solutions for optical solitary waves in nematic liquid crystals," *Physica D,* **284**, 1–15 (2014).

[26] M. Born and E. Wolf, "Principles of Optics," 7th edn, Cambridge University Press (1999).

[27] R.J. Potton, "Reciprocity in optics," *Rep. Progr. Phys.,* **67**, 717–754 (2004).

[28] A.T. De Hoop, "Reciprocity of the electromagnetic field," *Appl. Sci. Res.,* **8**, 135 (1959).

[29] D. Jalas et al., "What is — and what is not — an optical isolator," *Nature Photon.,* **7**, 579–582 (2013).

[30] Y. Shi, Z. Yu and S. Fan, "Limitations of nonlinear optical isolators due to dynamic reciprocity," *Nature Photon.,* **9**, 388–392 (2015).